Multilayer mirror based line emission tomography for spherical Tokamaks

D. Stutman, Y. S. Hwang, J. Menard, W. Choe, and M. Ono
Princeton Plasma Physics Laboratory, Princeton University, Princeton, New Jersey 08543

M. Finkenthal, M. J. May, S. P. Regan, V. Soukhanovskii, and H. W. Moos
Johns Hopkins University, Baltimore, Maryland 21218

(Presented on 16 May 1996)

Due to their highly shaped plasma and possible poloidal asymmetry in impurity concentration, spherical Tokamaks will require tomographic reconstruction of local emissivities to assess impurity content and transport. To collect in an effective manner the data required for such reconstruction, we develop arrays of high throughput ''mini-monochromators'' using extreme ultraviolet multilayer mirrors as dispersive elements and filtered surface barrier diodes as detectors. We discuss monochromator optimization and show that by working at near normal incidence throughput and spectral resolution are simultaneously maximized. A system proposed for tomographic reconstruction of C V and C VI resonance emission at 33.7 and 40.5 Å respectively, achieves 0.9 Å spectral resolution, 2 cm spatial resolution, and 0.2 ms temporal resolution, together with good sensitivity and background rejection. Preliminary results obtained from CDX-U low aspect ratio tokamak are also presented. © *1997 American Institute of Physics.* [S0034-6748(97)67301-3]

I. INTRODUCTION

Spherical Tokamaks (STs) having aspect ratio $R/a<1.5$ are proposed as an improvement of the Tokamak concept.[1] Preliminary experimental results from low aspect ratio machines are encouraging,[2,3] and several STs having plasma currents up to 1 MA [e.g., MAST at Culham, National Spherical Tokamak Experiment (NSTX) at Princeton Plasma Physics Laboratory (PPPL)] are being considered for construction.

The investigation of impurity effects may be even more important for ST than for conventional Tokamaks: noninductive start up and heating/current drive are essential for ST performance,[4] and such operation regimes can introduce significant amounts of impurities. However, several aspects may concur to make difficult the spectroscopic investigation. First, ST plasmas are very elongated (e.g., $\kappa\approx 2.2$ for NSTX), have large triangularity and Shafranov shifts, and a ''natural divertor'' configuration of the scrape-off layer. Second, impurity ion density might exhibit significant up/down and in/out poloidal asymmetries over the flux surfaces, making thus impossible the interpretation of chord integrated measurements.

Neo-classical transport theory predicts that impurity concentration asymmetries of the order of $\epsilon\equiv r/R$ can occur due to ∇B drifts and working ion/impurity ion friction.[5,6] Measurements in large aspect ratio Tokamaks substantiate these predictions up to quite large values of ϵ (≈ 0.3).[5,7] Although the theory is developed in the large aspect ratio approximation ($\epsilon\ll 1$) and cannot be used to predict the degree of asymmetry near the ST edge, it is interesting to try and estimate the magnitude of such effects closer to the ST axis where the above assumption is valid. Considering, for example, the NSTX plasma at $\epsilon=0.25$ ($R\approx 0.8$ m, $a\approx 0.65$ m), and using the model in Ref. 5 with parameters which may be projected at this radius (e.g., $T_i\approx 1$ keV, $N_i\approx 3\ 10^{13}$ cm^{-3}, $q(r)\approx 2$, $p_i/[r\,\partial p_i/\partial r]\approx 1.5$, $B_{\mathrm{TO}}\approx 0.5$ T), one obtains for instance for a highly charged ion such as He-like Ti (a probable impurity in NSTX due to TiC coated rf antenna shields) a very significant difference of about 30% in up/down concentrations, and an in/out difference of about 10%. Thus, in contrast with conventional Tokamaks, large poloidal asymmetries might exist in ST plasmas not only at the edge, but also deep inside the plasma.

A solution to the impurity diagnostic problem is to unfold the impurity line emissivity using 2D tomographic techniques, as is commonly done for reconstruction of energy integrated, soft x-ray emissivity.[8] To this end, XUV monochromators having high throughput, good spectral, spatial and temporal resolution, and absolute photometric calibration are needed. At the same time, they have to be sufficiently compact and inexpensive so that arrays with tens of elements can be constructed. In the present work, we show that such devices can be built using synthetic multilayer mirrors (MLMs) in conjunction with filtered surface barrier photodiodes, and exemplify with a dual tomography system for simultaneous reconstruction of the C VI $1s$-$2p$ emission at 33.7 Å and the C V $1s^2$-$1s2p$ emission around 40.5 Å. The system is proposed for the investigation of impurity transport in the CDX-U low aspect ratio Tokamak at PPPL.

II. C V/C VI MLM MONOCHROMATORS

Due to their simplicity and versatility, MLM based spectroscopic systems are increasingly used as fusion plasma diagnostics.[9] Here we discuss optimization of MLM monochromators for the 31.7 and 40.5 Å C emission. The main reason for choosing C V and C VI for an investigation of impurity transport in CDX-U is that we expect these ions to sample most of the plasma volume both in ohmic and auxiliary heated discharges. Also, their $1s-2p$ transitions are advantageous from the modeling point of view, since excitation is usually dominated by electron collisions and the rate coefficients are well known. We desire a simultaneous measurement of C V and C VI emission in order to eliminate the large uncertainties arising in modeling due to shot to shot variability.

The characteristics required for the monochromators derive from the above physics goal. Thus, as shown in a companion article,[10] spatial resolution $\leqslant 2$ cm at midplane is needed to resolve the gradients expected in CDX-U C V and C VI emission. Temporal resolution has to be some small fraction of the CDX-U impurity confinement time—which using conventional scaling we estimate to be between 4 and 8 ms. Spectral resolution around 1 Å is largely sufficient since we expect the spectral region between 30 and 50 Å to be free of other intense line emission. This enables using MLMs as dispersive elements, their theoretical resolution being $\approx 0.7-1$ Å at the wavelengths of interest. Finally, a requirement for maximal compactness arises from mechanical constraints near CDX-U vessel.

(1) Mutilayer mirrors: The physics of the multilayer mirrors is reviewed in Ref. 11. Most MLM based spectroscopic systems use highly collimated beams to achieve good spectral resolution and angles of incidence away from normal to benefit from large mirror reflectivity. These reduce the collected photon flux, and as a result, high gain detectors [photomultipliers (PMTs), channeltrons, etc.] have to be used to obtain useful signal levels. Such detectors, however, have low quantum efficiency and it is also very difficult and expensive to incorporate in large arrays (due to size, complexity, and shielding problems).

On the other hand, there is satisfactory experience with using Si photodiodes for Tokamak diagnostic.[8] These are simple, compact, relatively low cost, and easy to incorporate in arrays. Also, their high quantum efficiency enables good signal-to-noise ratio (SNR) even for short detection times. It is therefore attractive to use such detectors in conjunction with MLMs for line emission tomography. Since no internal gain is available, for MLM/photodiode monochromators it is essential to maximize the optical throughput together with spectral resolution. This is achieved by working at near normal incidence.

MLM reflectivity decreases with increasing incidence angle;[11] however, the angular width of the diffraction peak increases rapidly according to Bragg dispersion relation: $\Delta\theta_B = \Delta\lambda/\lambda_0 \tan\theta_B$, with $\Delta\theta_B$ the angular FWHM of the diffraction peak at Bragg angle θ_B, and $\Delta\lambda/\lambda_0$ the theoretical (infinitely narrow beam limit) wavelength resolution. Since the latter is nearly independent of the incidence angle, $\Delta\lambda/\lambda_0 \approx 1/N$, with N the number of effective reflective layers,[11] the $\tan\theta_B$ factor is determinant. Therefore, by working near normal incidence and using collimation of angular width $\Delta\theta_C \approx \Delta\theta_B$ one achieves simultaneously a large increase in geometrical étendue G (since $G \sim \Delta\theta_C^2 \approx 1/N \tan\theta_B^2$),and near theoretical wavelength resolution (since collimator broadening is not significant). A numerical example shows that the étendue increase at normal incidence is much larger than the reflectivity decrease.

We compare for example at $\lambda \approx 33.7$ Å the performance of series W/B_4C MLMs having $2d \approx 35$ Å and of Ti/Sc mirrors with $2d \approx 90$ Å. The respective peak reflectivities P_0, are about 1.8%[12] and 19% (our measurements), while wavelength resolution is similar, $\Delta\lambda/\lambda \approx 1/50$. Using the approximations from Ref. 13, we compute then for both mirrors the wavelength resolution $\Delta\lambda_C$, as a function of the monochromator collimation width $\Delta\theta_C$ (Fig. 1). It is seen that using the normal incidence geometry one can have both wide angle collimation and near theoretical spectral resolution. On the other hand, in order to obtain similar wavelength resolution at grazing incidence $\Delta\theta_C$ has to be reduced by about an order of magnitude. Thus, although reflectivity averaged over $\Delta\theta_C$ is about ten times higher for the grazing incidence mirror, the two orders of magnitude higher étendue at normal incidence makes the overall throughput about an order of magnitude larger.

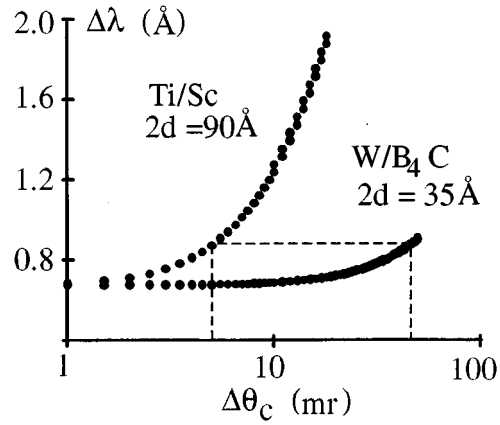

FIG. 1. Wavelength resolution for normal and grazing incidence MLM monochromators as a function of collimation angular width.

We choose therefore W/B_4C mirrors having $2d \approx 35$ Å, $P_0 \approx 1.8\%$ and $2d \approx 42$ Å, $P_0 \approx 2\%$ for the C VI and C V monochromators, respectively.[12] For increased étendue, we use rectangular collimation of dimensions $6.5 \times 28 \times 140$ mm, with the 28 mm side along toroidal direction. (Cross sectional dimensions are determined by the photodiode active area.) With the entrance aperture at 5 cm behind limiter radius, this geometry provides a high étendue of $1.8\ 10^{-2}$ cm^2 sr, spectral resolution of ≈ 0.9 and 1.1 Å at 33.7 and 40.5 Å, respectively, and spatial resolution of ≈ 2 cm at midplane.

(2) Background rejection filters: Since the VUV to EUV CDX-U emission is about two orders of magnitude brighter than the 31.7 and 40.5 Å emission, and MLM long wavelength specular reflectivity is larger than Bragg reflectivity, strong rejection of light above ≈ 100 Å is mandatory for our system, simultaneous with maximum transmission at 30–40 Å. Our experience shows that this can be achieved using M-edge elemental filters. In the present case, we choose Sn, for its superior blocking properties in the critical region between $\approx 100-150$ Å where bright O VI emission occurs in CDX-U. However, since Sn has a transmission window in the EUV, we use a composite filter consisting of 1000 Å Sn and 1000 Å Ti; Ti has excellent transmission between 30–40 Å, while efficiently "plugging" the tin EUV window. The resulting transmission[14] including a 200 Å gold layer on the surface barrier diode is plotted in Fig. 2 and shows that better than 10^5 background rejection is achieved.

(3) Photodiode and amplifiers: Using the above data we obtain the sensitivity of the monochromators as: I [nA]$\approx 1.25\ B/10^{12}$ at 40.5 Å and $\approx 1.4\ B/10^{12}$ at 33.7 Å, where B is source brightness in photons/cm^2 sr s. Since expected

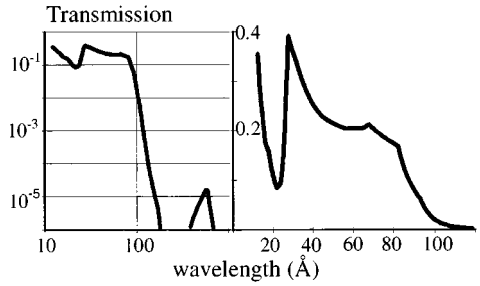

FIG. 2. Transmission of Sn/Ti filter used with C V/C VI MLM monochromators.

brightness is from a few times 10^{12} at the edge, up to 10^{14} photons/cm^2 sr s at midplane,[10] the diode currents are from a few nA to ≈100 nA. While the currents at midplane can be easily measured, a few nA levels require optimization of diodes and amplifiers for minimal noise, pick up, and fastest response.

We tested 1 cm^2 active area, absolute XUV photodiodes [planar mount AXUV-100 from International Radiation Detectors (IRD) and coaxial mount XUV-100 from United Detector Technology (UDT)], as well as 7×30 mm rectangular surface barrier diodes (SBDs) produced by EG&G Ortec. We found that SBDs perform best in terms of noise, bandwidth, and pick-up immunity, most probably due to lower capacitance and the intrinsic coaxial construction. The pick-up level during plasma shots at $I_p \approx 60$ kA did not exceed 0.5 nA at 10^8 V/A transimpedance gain. Therefore, despite some signal attenuation in the 200 Å gold contact, SBDs seem to be the best suited detectors for our MLM based monochromators.

Low noise, high gain, and fast amplifiers are an important part of the proposed system. Using the simple circuit in Ref. 10, operated at 10^8 V/A gain and the Ortec SBDs, we achieve ≈5:1 SNR and ≈2–3 kHz bandwidth for 0.5 nA amplitude signals. Thus, the performance of our monochromators is apparently limited by diode pick up. Assuming this limit, the lowest measurable brightness at 30–40 Å is around 1–2 10^{12} photons/cm^2 sr s, for a bandwidth of a few kHz. This is comparable to the sensitivity of conventional XUV instruments using high gain detectors.

(4) Photometric calibration: For impurity content determination, absolute photometric calibration of the monochromators is required. In comparison with conventional XUV monochromators, this is a relatively simple task for the MLM/diode instrument, since its components can be individually calibrated using either synchrotron radiation or line sources. The components are also much less sensitive to contamination and instrument response is very stable over long period of times.

III. MONOCHROMATOR ARRAYS FOR CDX-U AND PRELIMINARY RESULTS

The rectangular cross section of CDX-U vacuum vessel permits designing the monochromator arrays with parallel lines of sight [Fig. 3(a) and 3(b)]; this is different from most Tokamak tomography systems, and offers the advantage that

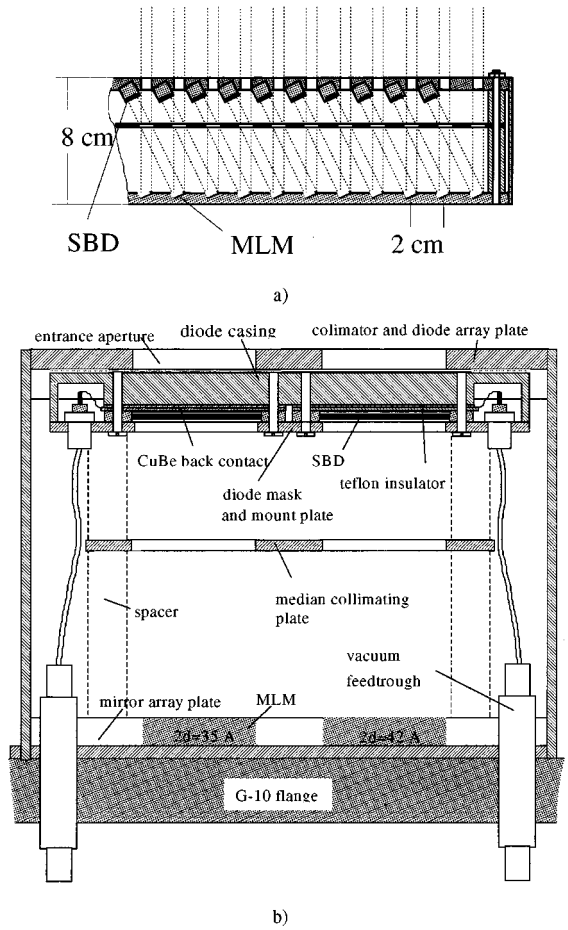

FIG. 3. Schematic of dual MLM/SBD tomographic array.

reconstruction is simplified on a regularly spaced grid. In addition, since spectral resolution and background rejection are sufficient to warrant spectral purity without the need for wavelength scanning, we design the arrays using fixed position mirrors and detectors. To achieve a very compact layout of ≈8 cm height, we place the MLMs at middistance between entrance and exit aperture (diode face). Also, by interspersing the monochromators as shown in Fig. 3(a), we obtain the required 2 cm spacing between monochromators. A median collimating plate is used to eliminate crosstalk between channels. Finally, using mirrors with the above $2d$ spacing the Bragg angles for the 33.7 and 40.5 Å transitions are the same. This enables pairing the two sets of mirrors and their associated diodes on the same array for the simultaneous detection of C V and C VI lines.

Since small $2d$ spacing W/B_4C mirrors were not available at the time of the experiment, to test the near normal incidence, MLM/photodiode monochromator concept we utilized $2d \approx 190$ Å Mo/Si mirrors and AXUV-100 diodes with 2 kÅ Al coating. Using such an instrument, we measured the O VI $2p-3d$ lines around 170 Å, while simultaneously recording with a conventional grating monochromator equipped with PMT detection the $2s-2p$ emission of the same ion at $\lambda \approx 1032$ Å. Figure 4 illustrates the main difference between the two instruments: although the time histories of the two lines are on the whole similar, the very high throughput and quantum efficiency of the MLM/photodiode

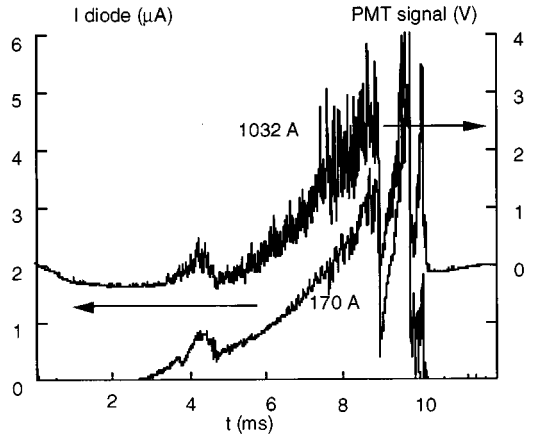

FIG. 4. Comparison between O VI emission from CDX-U recorded at 170 Å using an MLM/photodiode monochromator and at 1032 Å emission using a conventional grating instrument equipped with phosphor/PMT detection.

monochromator enables clear observation of magnetohydrodynamics (MHD) induced fluctuations on the O VI signal. With the conventional monochromator on the other hand, the MHD fluctuations are masked by the large statistical fluctuations in the number of recorded photoelectrons.

IV. CONCLUSION

We propose to use for tomographic reconstruction of impurity line emission from ST arrays of multilayer mirror/photodiode monochromators. We show that working at near normal incidence, high throughput, and compact devices can be realized for the difficult spectral region between 30–40 Å. Preliminary results from CDX-U demonstrate that richer physical information can be gained with such instruments than with conventional ones.

ACKNOWLEDGMENTS

The authors acknowledge Dr. S. von Goeler for kindly providing the SBDs for the experiment. This work is supported by DOE Contract No. DE-AC02-76-CHO-3073 at PPPL and DOE Grant No. DE-FG02-86ER52314AT at Johns Hopkins University.

[1] Y.-K. Peng and D. J. Strickler, Nucl. Fusion **26**, 769 (1986).
[2] A. Sykes *et al.*, Plasma Phys. Control. Fusion **35**, 1051 (1993).
[3] Y.-S Hwang *et al.*, in *Proceedings of the 22nd EPS Conference on Controlled Fusion and Plasma Physics, Bournemouth* (EPS, Bournemouth, 1995), Vol. II, p. 93.
[4] M. Ono, Phys. Plasmas **2**, 4075 (1995).
[5] W. Feneberg *et al.*, Rep. JET-R(86)07, JET Joint Undertaking, Abingdon, Oxforshire, 1986 (unpublished).
[6] C. T. Hsu and D. J. Sigmar, Plasma Phys. Control. Fusion **32**, 499 (1990).
[7] R. D. Durst, Nucl. Fusion **32**, 2238 (1992).
[8] S. von Goeler, in *Diagnostics for Fusion Experiments* (Pergamon, New York, 1979), p. 79.
[9] S. P. Regan *et al.*, Rev. Sci. Instrum., these proceedings.
[10] D. Stutman *et al.*, Rev. Sci. Instrum., these proceedings.
[11] B. L. Henke *et al.*, J. X-ray Sci. Technol. **2**, 17 (1990).
[12] G. Gutman, J. X-ray Sci. Technol. **4**, 142 (1994).
[13] B. L. Henke, *Low Energy Diagnostics, Monterey CA, 1981*, edited by D. T. Attwood and B. L. Henke, AIP Conf. Proc. No. 75 (AIP, New York, 1981), p. 85.
[14] B. L. Henke *et al.*, At. Data Nucl. Data Tables **54**, 205 (1993).